Development and Validation of a New Detailed EMT-type Component-based Load Model

M. Torabi Milani, B. Khodabakhchian, J. Mahseredjian, K. Sheshyekani

***Abstract*--Load modeling is one of the most important parts in power system simulation. This paper describes the efforts to develop a detailed EMT-type component-based load model. The aim of this new model is to capture the accurate behavior of loads in commercial and residential sectors. The developed model is validated and refined against field data which were recorded by Hydro-Quebec during voltage sag events. The simulations are performed using the time-domain simulation tool EMTP.**

***Keywords*: Component-based, EMTP simulation, Load modeling.**

I. Introduction

LOAD modeling is one of the most important areas in power system modeling. Previous research has reported discrepancies between the recorded and simulated system responses as a result of employing incorrect load models. Examples are several unsuccessful attempts to reproduce the behavior observed in the Swedish blackout in 1983 [1], the Tokyo network collapse of 1987 [2] and the Western Systems Coordinating Council (WSCC) blackout in 1996 [3]. Accordingly, accurate analysis of power systems requires accurate load models.

Load models can be divided into two basic groups, being static and dynamic. Static models describe the load characteristics with respect to voltage and frequency variations assuming no machine dynamics. Existing static models such as exponential load model, polynomial load model (ZIP) and linear load model are described in [4] and [5]. Various existing dynamic load models including exponential dynamic load model and dynamic models of induction motor have been presented in [4]. Composite load models can represent the structure of a given load as a combination of static and dynamic load components. The most common composite load model is the combination of an induction motor model and a static load. In [6] and [7], the static part is represented with a conductance and a susceptance in parallel. A ZIP model has been used in [5] and [8] to represent the static component.

To represent aggregated loads at power system buses, two most widely used methodologies exist; the measurement-based and the component-based approach. In the former, load characteristics are derived based on measurements performed in the actual power system. In the latter however, a load model is constructed from the models of the individual load components. Examples of measurement-based approach are available in [9] and [10]. Component-based approach has been reported in [11], [12] and [13] to develop aggregated household, industrial and residential-commercial loads respectively.

Although the importance of load modeling is generally recognized and different load modeling efforts have been documented in existing literature, little has been done to develop detailed composite load models. Such models provide a more accurate representation of the reality of aggregated loads, as they recognize the diversity in end-use characteristics (e.g., different types of motors and lighting sources). The research papers available on detailed composite load models are [13] and [14]. The latest development in this field belongs to the composite load model (CMLD) in PSSE [14]. This model is an aggregation of three-phase and single-phase induction motors, power electronics and static loads. However, it suffers from inaccuracy in modeling power electronics and single-phase motors; power electronics are grouped as constant power loads which is a simplistic assumption. The single-phase motor is approximated by a "performance model" using algebraic equations to represent the motor power consumption in terms of terminal voltage.

This paper presents a new detailed component-based load model based on electromagnetic transient (EMT) computations. The aim of this model is to approach the real load behavior under disturbances, e.g., voltage variations. The new model not only captures the diversity in end-use applications, but also includes modern elements such as variable speed drives and energy efficient lighting sources. To the author's best knowledge, such a comprehensive EMT-type load model has not been previously presented in the literature. The developed model is used to simulate load behavior in voltage variation events, and its performance is validated against field data recorded by Hydro-Quebec. Results of the validation studies reveal the capability of the proposed model in reproducing the measured dynamic behaviour of loads during and after a disturbance. Obtaining such results is not possible by employing traditional load models, especially static ones which are the current practice in most dynamic studies [4]. Moreover, in this paper, measured data is also used to derive relevant characteristics of the modelled loads (e.g., connection or reconnection pattern of motor loads during and following voltage sags) which are subsequently exploited in

M. Torabi Milani, J. Mahseredjian and K.Sheshyekani are with Polytechnique Montreal, Montreal, QC H3C 3A7, Canada (e-mail: maryam.torabi@polymtl.ca; jean.mahseredjian@polymtl.ca; keyhan.sheshyekani@polymtl.ca).
B. Khodabakhchian is with Hydro-Quebec, Montreal, QC H5B 1H7, Canada (e-mail: khodabakhchian.bahram@hydroquebec.com).

Paper submitted to the International Conference on Power Systems Transients (IPST2021) in Belo Horizonte, Brazil June 6-10, 2021.

the development and practice of the proposed model. This combination of measurement-based and component-based approaches is another technical contribution of this work; not only it provides a more realistic representation of load characteristics, but also offers some insight into general considerations when modeling similar types of loads.

This paper is organized as follows. Section II describes the new load model and elaborates its different components. Validation of the developed model in two load sectors namely commercial and residential is presented in section III using the field recordings provided by Hydro-Quebec.

II. The Component-Based Load Model

The new load model is developed in a component-based aggregation procedure, as depicted in the schematic of Fig. 1. The model is subdivided into several components which represent electrical devices found within end-use applications. The circuit-based model of each component is built in EMTP (when required, the component models are adopted from previous research in the literature). Component models are developed using per-unit parameters which allows the aggregation of individual loads according to their percentage contribution in the total demand. Those individual models are then aggregated to form the complete load at the distribution bus. An aggregation procedure with such high level of details has not been found in the existing literature. The component models are elaborated as follows.

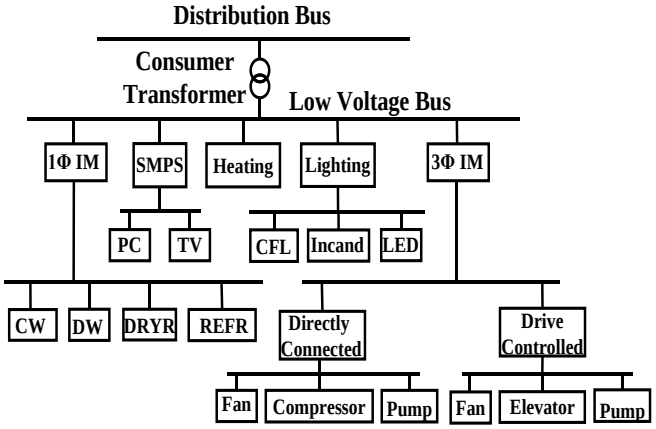

Fig. 1. Structure of the aggregated load model using component-based technique

Incandescent lamps (Incand), heaters and water heating elements are modeled as voltage dependent and constant resistance loads, respectively.

Switch mode power supply loads (SMPS) i.e., TVs and PCs are modeled as shown in Fig. 2 [15]. The equivalent resistance is presented in Table I. The typical per-unit value of C_{dc} is 0.036 pu (reactance) [15].

TABLE I
Equivalent Resistance of SMPS and CFL

Component	R_{eq}
SMPS	$R_{eq} = \frac{v_{dc}^2}{P_{rated}}$
CFL	$R_{eq,charging} = 11v_{dc} + 0.021v_{dc}^2 + 1300$ $R_{eq,discharging} = 23.7v_{dc} + 274$

Compact fluorescent lamps (CFL) are represented by the circuit of Fig. 2 and the equivalent resistance is defined in Table I based on the charging or discharging state of the capacitor [15].

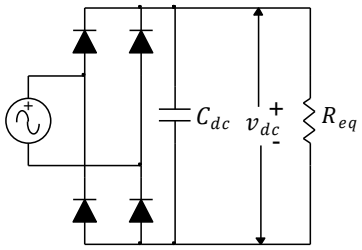

Fig. 2. SMPS circuit topology

Light emitting diodes (LEDs) are represented by a linear model consisting of a threshold voltage in series with a dynamic resistance (V_{thr}=2.7 V, R_d= 0.3 Ω). A driver circuit is employed to regulate LED currents and provide a stable lighting output [16]. Fig. 3 presents a driver circuit consisting of a front-end rectifier (ideal models are utilized for diodes), dc link capacitor and a fly-back dc-dc converter which is used to supply 30 W LED modules. C_{dc} is 0.036 pu (reactance).

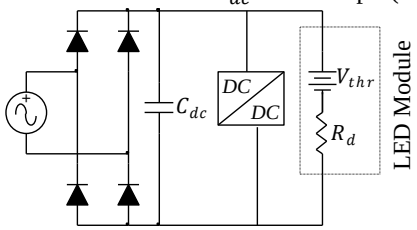

Fig. 3. LED driver circuit topology

Elevators and compressors are modeled as three-phase induction motors (IM) with constant torque mechanical load characteristics. To reasonably model the motor loads, realistic parameters should be used. The corresponding per-unit parameters are taken from [14].

Fans and pumps are modeled as three-phase induction motors with quadratic torque load characteristics. The per-unit parameter related to this category is taken from [14].

Variable frequency drives for three-phase induction motors are implemented using a pulse-width-modulation (PWM) controlled voltage source inverter (VSI) and vector control (field-oriented control) technique.

Refrigerator/freezers (REFR), dishwashers (DW) and cloth washers (CW) are modeled as single-phase induction motors driving quadratic torque loads. Cloth dryers (DRYR) are modeled as 30% single-phase induction motor and 70% resistive element. This type of motor has quadratic torque load characteristics. More details on the characteristics of single-phase motors are given in section III. B.

Fig. 1 is developed in EMTP using subcircuits. This is a hierarchical way of representation which provides high-level access to subcircuit contents using masks and scripts. In the top-level mask, the following parameters are specified as user-defined values: voltage level of the distribution bus, total power demand, percentage contribution of individual load components, and proportion of motor loads controlled with variable speed drives. The individual component models which are placed inside the subcircuit are aggregated based on

their percentage contribution specified in the mask. The aim of this scripted subcircuit is to provide a generic and flexible load representation which offers the possibility of being used in any network and any load sector (i.e., residential, commercial and small industrial).

III. Validation of the Developed Load Model

In this section, three case studies are presented which validate the developed model in commercial and residential load sectors. Results of the case studies are further discussed at the end of this section.

A. Commercial Load

In the commercial sector, a recorded event at a shopping mall in Montreal is reproduced by using the developed model. The recorded voltage waveforms resulted from a disturbance that lasted for 0.296 s and provoked following voltage drops on the three phases: 67.9% voltage drop on phase a, 64% voltage drop on phase b and 62.8% voltage drop on phase c of a 12.47 kV system (see Fig. 4, solid lines). An adjusted ideal voltage source is used to reproduce the recorded instantaneous voltages (see Fig. 4, dotted lines). The event is simulated by applying the voltage source to the developed model of the shopping mall as explained in section II.

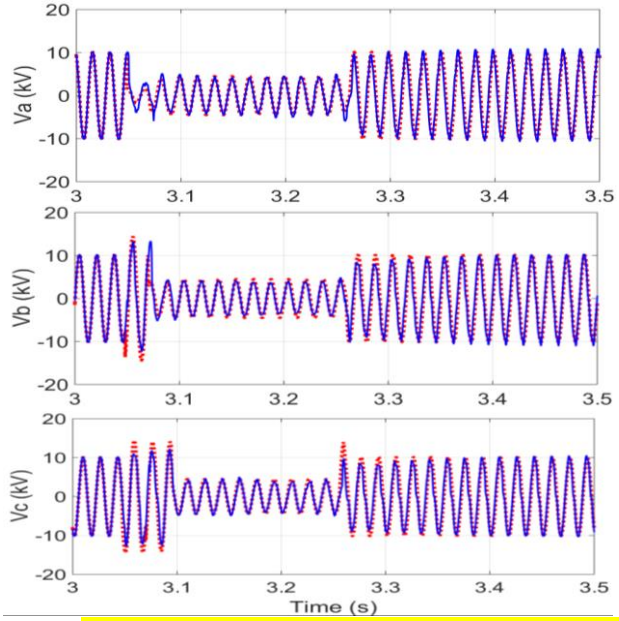

Fig. 4 Three-phase voltages; simulation (dotted) vs measurement (solid) related to the commercial load case study

This shopping mall had a 1.52 MW pre-fault load. Load composition is strongly dependent on the geographic location, time, and also temperature. Since no information is available on the composition of this load, first some assumptions are made based on the typical usage of a commercial center at the time of the event, 11:46 September 29th, 2020. Next, further adjustments are made in the load composition to match the simulation results with the measured signals as closely as possible. The considered composition which provides the best match to the recordings is listed in Table II.

Fig. 5 presents the comparison between simulated results and recorded data for three-phase currents. Active and reactive power demands comparisons are presented in Fig. 6.

TABLE II
Commercial Load Composition

Component	Composition	Component	Composition
Compressor	8%	CFL	20%
Pump	10%	Incandescent	0%
Fan	20%	LED	20%
Elevator	0%	SMPS	15%
1φ Motor	5%	Cooking	2%

Analyzing the measured signals yields the following points which are applied in the simulations. The best agreement is achieved between the simulated and recorded currents in terms of harmonic contents by making all motors to be directly connected. Voltage sag may induce loss of load in the system. Contactors of motor loads drop out at voltage levels around 45-55% of nominal voltage in about 1-3 cycles [14]. In this case study, all motor loads are tripped during simulation of the voltage sag. The low currents observed during the fault are attributed to this loss of load. When voltage recovers to about 65% of the nominal value, motor contactor will reclose within few cycles [14]. Reconnection of 70% of motors 20 ms after voltage recovery provides the best match to the recorded currents. The observed inrush current (see Fig. 5 near 3.3 s) at the time of voltage recovery is due to reconnection of motors. It should be noted that dropping of motors during voltage sag and their reconnection after voltage recovery cannot be generalized and depends on the controls and protection parameters associated to each motor load.

As noticed, the simulation results are sufficiently accurate when compared against measurements, but it is always difficult to match reactive power more accurately.

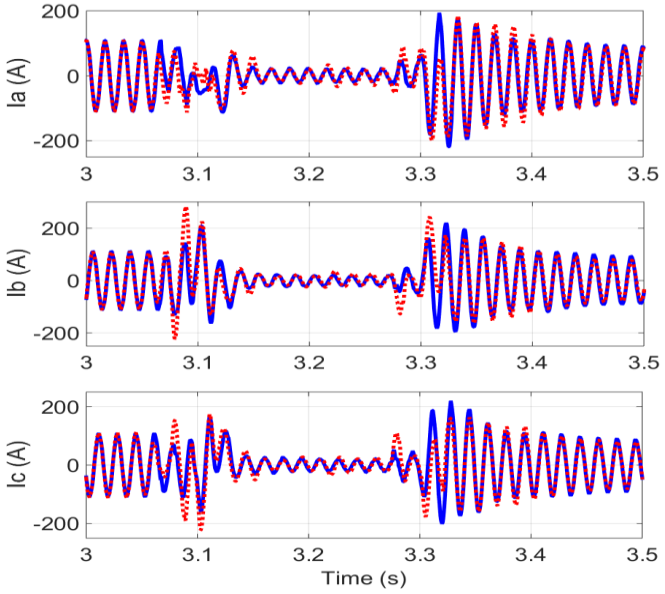

Fig. 5. Three-phase currents; simulation (dotted) vs measurement (solid) related to the commercial load case study

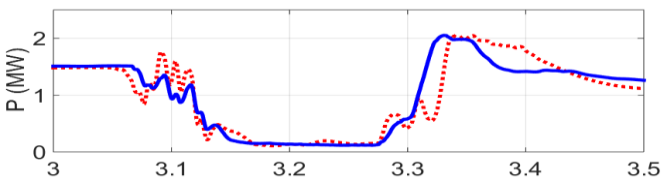

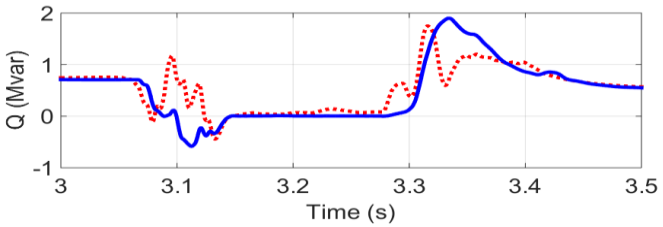

Fig. 6. Active and reactive power; simulation (dotted) vs measurement (solid) related to the commercial load case study

B. Residential Load

The validity of the proposed model in the residential sector is demonstrated by reproducing two available event recordings for faults in a specific area in Montreal which is supplied by a local distribution company. Google Earth application [17] has been used in order to identify the type and number of consumers in this area; about 600 houses and one small industry.

Event 1

The first event is recorded on 8:50 August 21st, 2020. At this time of the day, no major activities are expected from the industrial consumer, so the whole consumption is attributed to the residential sector. The load composition related to 4.5 MW pre-fault load is listed in Table III based on the information provided in [18] for typical residential consumption at the time of this event.

TABLE III
RESIDENTIAL LOAD COMPOSITION, EVENT 1

Component	Composition	Component	Composition
Water heater	16%	Refrigerator	15%
Lighting	10%	Dish washer	5%
TV+PC	32%	Washer	2%
cooking	10%	Dryer	10%

Voltage measurements show 66.8% voltage drop on phase a, 66.6% voltage drop on phase b, and 65.7% voltage drop on phase c as the result of a fault which lasts for 0.8 seconds (voltage recordings related to this fault are available similar to what is shown in Fig. 4 and are not presented for this case study). The actual measured voltages are reproduced by imposing faults on the three phases as shown in schematic of Fig. 7. Based on the provided single-line diagram by Hydro-Quebec, this residential load is supplied from a 230/25 kV substation.

Since the dynamic behavior of a residential load is governed by its single-phase motors, a significant point in this simulation is the selection of realistic parameters for modeling those motor loads. Motor parameters related to different end-use applications are taken from [4]. Although some references have addressed the load torque characteristics attributed to different types of single-phase motors, some disagreement can be seen between the available information. While [18] has presented refrigerator motors as constant torque mechanical load type, [15] has referred to them as quadratic torque. While washers, dish washers and dryers are considered as quadratic torque mechanical load type in [15], the same motors are considered as constant torque type in [18]. Several simulations were performed using different types of mechanical loading for each sing-phase motor and the results showed that quadratic torque mechanical load types reproduce the measured behavior more realistically. The comparison between simulated results and recordings for three-phase currents and powers are presented in Fig. 8 and Fig. 9 respectively. It should be noted that no loss of load is observed in this case.

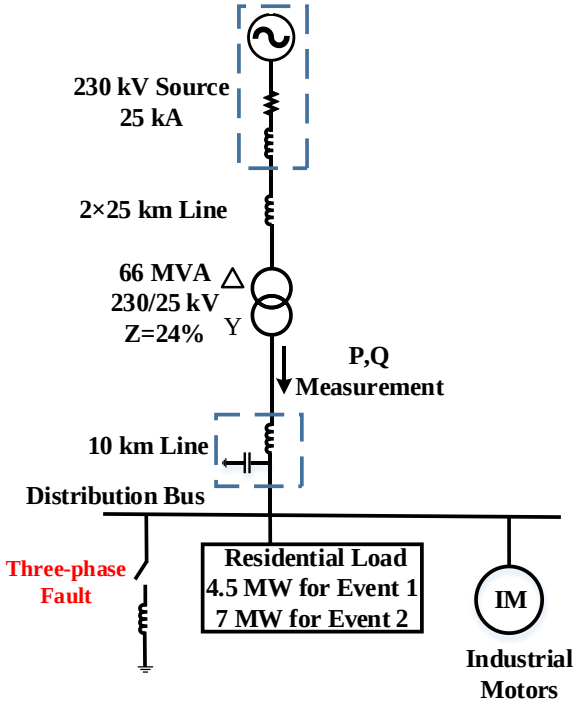

Fig. 7. Single-line diagram of the residential load case study

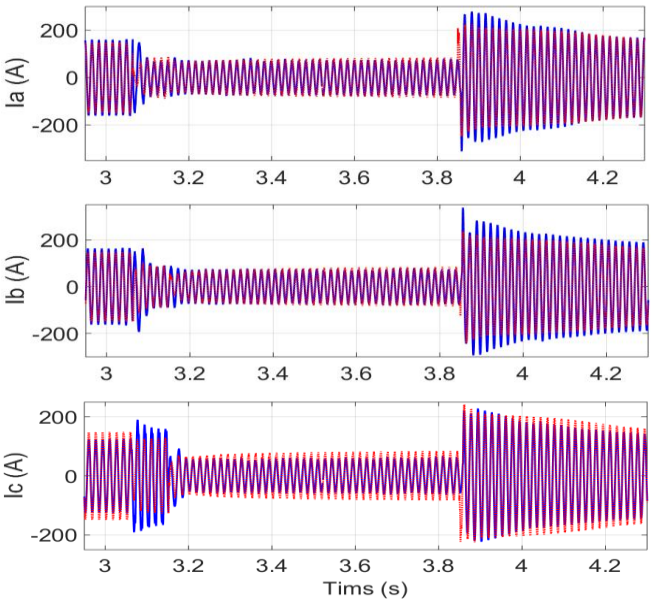

Fig. 8. Three-phase currents; simulation (dotted) vs measurement (solid) related to the residential load case study, Event 1

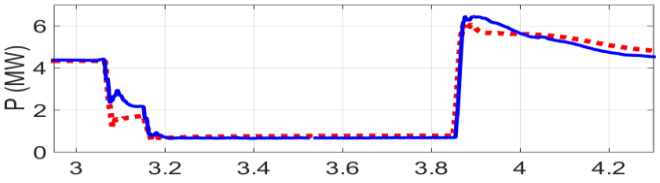

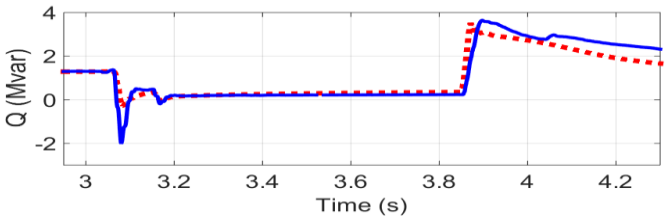

Fig. 9. Active and reactive power; simulation (dotted) vs measurement (solid) related to the residential load case study, Event 1

Event 2

The second recorded event is also related to the network of Fig. 7 but at a different time, 16:17 April 4th, 2020. At the time of this event, some contribution should be expected from the industrial load. Based on the recorded active powers (post-fault power of 5.5 MW versus 7 MW pre-fault power), it can be noticed that some of the load is lost as the result of the voltage sag. This observation is an indication of the presence of 1.5 MW industrial motors which have been tripped during the voltage sag. Therefore, the load mix is considered to be 20% industrial motors and 80% residential loads. The load composition related to the residential load class is assumed as Table IV based on the information provided in [18].

TABLE IV
RESIDENTIAL LOAD COMPOSITION, EVENT 2

Component	Composition	Component	Composition
Water heater	10%	Refrigerator	15%
Lighting	5%	Dish washer	5%
TV+PC	30%	Washer	5%
cooking	20%	Dryer	10%

This event involves a disturbance which lasts for 0.7 seconds and causes 52.8% voltage drop on phase a, 53.5% voltage drop on phase b, and 54.7% voltage drop on phase c. In the same way as the previous case, the actual measured voltages are reproduced by imposing faults on the three phases as shown in schematic of Fig. 7. In this case study, the fault on phase a has started 12 cycles after the two other phases. To account for the load loss, the industrial motors are tripped 3 cycles after the beginning of the voltage sag. The comparison between simulated results and recordings for three-phase currents and powers are presented in Fig. 10 and Fig. 11, respectively.

C. Discussion on results

The results of the above three presented case studies show that the developed model can almost accurately reproduce the recorded waveforms in both residential and commercial load sectors. This implies that the new model is capable to predict the actual load behavior. Obtaining such results is not possible by employing traditional load models, especially static ones which are the current practice in most dynamic studies. This is because it is observed that dynamic characteristics of different single-phase and three-phase motors as well as their eventual tripping, play an important role to replicate load dynamics during and following a disturbance. The lack of dynamic motor models in traditional load models is the main cause of differences in results between field measurements and simulations. Furthermore, combining measurement-based and component-based approaches to derive additional characteristics of the modelled loads (e.g., connection or reconnection pattern of motor loads during and following voltage sags or load torque characteristics of single-phase motors) is beneficial. It moves simulation results closer to the recorded dynamics and thus provides a more realistic representation of loads.

These observations provide the validation of the developed model and verify that it can be utilized for modeling similar loads in dynamic studies even with large voltage variations or during asymmetrical faults. Moreover, it can be concluded, that approximate, yet reasonable load composition can reproduce the actual measured responses. All circumstantial data (i.e., geographical location, time, temperature, etc.) should be accounted for to achieve the best estimate of load composition. Nevertheless, load component data will always have some uncertainty no matter how hard one tries to obtain this information.

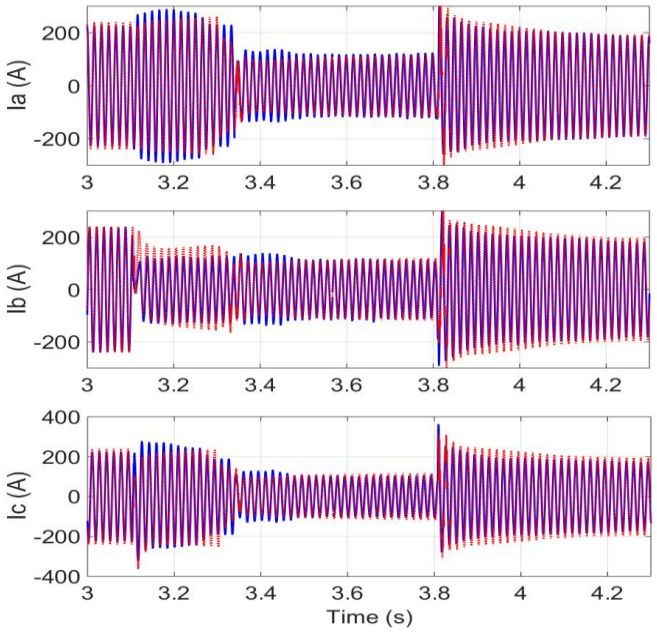

Fig. 10. Three-phase currents; simulation (dotted) vs measurement (solid) related to the residential load case study, Event 2

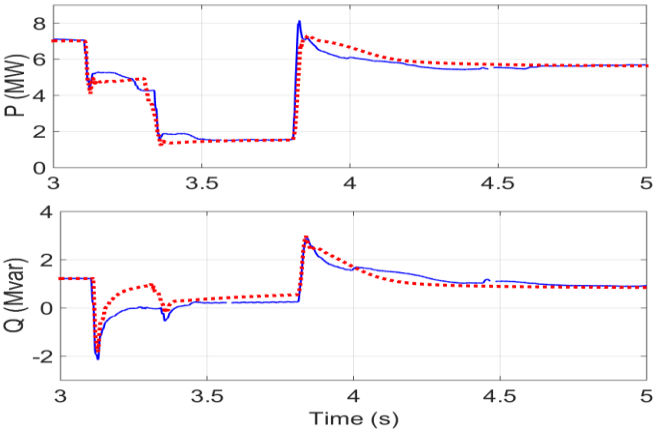

Fig. 11. Active and reactive power; simulation (dotted) vs measurement (solid) related to the residential load case study, Event 2

IV. CONCLUSION

In this paper, a detailed EMT-type component-based load

model is developed. Simulation results of three voltage sag events validate the performance of the new model in commercial and residential load sectors by comparing the simulated load responses against field data recorded by Hydro-Quebec. The measured data is also used to derive relevant characteristics of loads and apply them in the modeling process. This combination of measurement-based and component-based approaches is shown to provide more realistic representation of load behavior. The results also confirm that the developed model is valid for large voltage variations and can be utilized for modeling similar loads in dynamic studies.

V. References

[1] D. J. Hill, "Nonlinear dynamic load models with recovery for voltage stability studies," *IEEE transactions on power systems*, vol. 8, pp. 166-176, 1993.

[2] A. Kurita and T. Sakurai, "The power system failure on July 23, 1987 in Tokyo," *Proceedings of the 27th IEEE Conference* , pp. 2093-2097, 1988.

[3] D. N. Kosterev, C. W. Taylor and W. A. Mittelstadt, "Model validation for the August 10, 1996 WSCC system outage," *IEEE transactions on power systems*, vol. 14, pp. 967-979, 1999.

[4] Working group C4.605, "Modelling and aggregation of loads in flexible power networks," *Cigre*, 2014.

[5] Y. Zhu, Power System Loads and Power System Stability, Springer Nature, 2020.

[6] T. Y. J. Lem and R. T. H. Alden, "Comparison of experimental and aggregate induction motor responses," *IEEE Transactions on Power Systems*, vol. 9, no. 4, pp. 1895-1994.

[7] S. A. Y. Sabir and D. c. Lee, "Dynamic Load Models Derived from Date Acquired During System Transients," *IEEE Transactions on Power Apparatus and Systems*, Vols. PAS-101, no. 9, pp. 3365-3372, Sep.1982.

[8] H. Renmu, M. Jin and D. J. Hill, "Composite Load Modeling via Measurement Approach," *IEEE Transactions on Power Systems*, vol. 21, no. 2, pp. 663-672, May 2006.

[9] B.-K. Choi, H.-D. Chiang, Y. Li and H. Li, "Measurement-based dynamic load models: Derivation, comparison, and validation," *IEEE Transactions on Power Systems*, vol. 21, no. 3, pp. 1276-1283, 2006.

[10] X. Qu, X. Li, J. Song and C. He, "An Extended Composite Load Model Taking Account of Distribution Network," *IEEE Transactions on Power Systems*, vol. 33, no. 6, pp. 7317-7320, 2018.

[11] A. J. Collin, G. Tsagarakis and A. E. Kiprakis, "Development of Low-Voltage Load Models for the Residential Load Sector," *IEEE Transactions on Power systems*, vol. 29, no. 5, pp. 2180-2188, 2014.

[12] X. Liang, "A New Composite Load Model Structure for Industrial Facilities," *IEEE Transactions on Industry Applications* , vol. 52, no. 6, pp. 4601-4609, 2016.

[13] B. Khodabakhchian and G.-T. Vuong, "Modeling a mixed residential-commercial load for simulations involving large disturbances," *IEEE Transactions on power Systems*, vol. 12, pp. 791-796, 1997.

[14] NERC load modeling task force, "Technical reference document dynamic load modeling," 2016.

[15] C. Cresswell, "Steady state load models for power system analysis," Ph.D dissertation, Dept. Elect. Eng, Univ. of Edinburg, Edindurg, 2009.

[16] M. Arias, A. Vázquez and J. Sebastián, "An overview of the AC-DC and DC-DC converters for LED lighting applications," *automatika*, vol. 53, pp. 156-172, 2012.

[17] "https://www.google.com/earth/," [Online].

[18] A. J. Collin, "Advanced load modelling for power system studies," Ph.D dissertation, Dept. Elect. Eng. , Univ. of Edinburg, Edinburg, 2013.